

THE ULTRAVIOLET AND VISIBLE LIGHT VARIABILITY OF BP TAURI: POSSIBLE CLUES FOR THE ORIGIN OF T TAURI STAR ACTIVITY

THEODORE SIMON^{a)}

University of Hawaii, Institute for Astronomy, 2680 Woodlawn Drive, Honolulu, Hawaii 96822

FREDERICK J. VRBA

U.S. Naval Observatory, Flagstaff Station, P.O. Box 1149, Flagstaff, Arizona 86002

WILLIAM HERBST

Wesleyan University, Astronomy Department, Middletown, Connecticut 06457

Received 8 March 1990; revised 13 August 1990

ABSTRACT

BP Tau is a moderate-strength T Tauri star, which has previously been studied photometrically by Vrba *et al.* and shown to have a 7.6-day light cycle. We have re-observed BP Tau in order to monitor this star with the *IUE* satellite. In conjunction with the UV spectroscopy, we have also obtained nearly simultaneous ground-based optical photometry. At optical wavelengths, we initially found the star to be varying with a period of 7.6 days. This variability suddenly vanished and was followed by a quiescent state that lasted about 11 days. The star then resumed its variability with a period of about 6.1 days. The UV continuum and most of the UV emission lines appeared to vary in phase with the optical flux. No variations were observed on the very short timescales ranging from several hours to half a day expected on the basis of axisymmetric, quasi-steady-state accretion disk models of T Tauri stars. However, the nearly week-long variations we have observed may be consistent with a magnetically buffered accretion model, which has been proposed by Uchida and Shibata.

I. INTRODUCTION

The T Tauri stars (TTS) are well-known for their irregular photometric variability. However, a growing number of TTS are also known to show cyclic changes in brightness (e.g., Bouvier *et al.* 1986a; Bouvier and Bertout 1989; Herbst *et al.* 1986; Herbst 1989; Vrba *et al.* 1986, 1989). Included among these periodic variables is the mild TTS BP Tau, which in October 1983 exhibited a 7.6 day period over a broad range of wavelengths from 3600 to 8000 Å (Vrba *et al.* 1986). The full amplitude of these light variations increased from 0.1 mag at the longest wavelengths to nearly 0.8 mag at the shortest. By analogy with the chromospherically active BY Draconis and RS CVn-type stars, the variability of BP Tau and of the other periodic TTS has been attributed to an uneven distribution of starspots over the stellar surface, which modulates the brightness of the star as it rotates (Holtzman and Herbst 1986; Bouvier and Bertout 1989; Vrba *et al.* 1989). In the case of BP Tau, the rate at which the amplitude of variability increases toward shorter wavelengths indicates that the starspots must be hotter than the photosphere, rather than cooler, as is generally true for the more highly evolved spotted stars.

The optical spectrum of BP Tau, like those of other TTS, is marked by bright emission lines and a strong veiling emission at wavelengths below 4000 Å (e.g., Rydgren, Strom, and Strom 1976). Over the years, many explanations have been offered for these peculiarities of TTS spectra. Recent attention has focused on two main theories, the so-called deep chromosphere hypothesis and the accretion disk model.

In the deep chromosphere model, as it was originally pro-

posed by Herbig (1970), the excess continuum and line emission is the result of magnetic activity, which is a much more intense version of the activity that occurs on the surface of the Sun. Deep chromosphere models have been computed for BP Tau and other TTS by Calvet, Basri, and Kuhl (1984) and by Calvet and Marin (1987). To order of magnitude, the models for BP Tau reproduce the strengths of its Ca II *H* and *K* lines, the Mg II *h* and *k* lines, and the UV continuum excess. However, they fail to reproduce the profiles of the bright hydrogen lines, which are the hallmark of all TTS spectra, and accordingly these lines would require another mechanism for their formation, e.g., an expanding stellar envelope or wind (Kuhl 1964).

In the accretion disk model, the TTS owe their unusual spectra to circumstellar disks that survive from the earliest epoch of star formation. Axisymmetric, steady-state accretion disk models have been computed for BP Tau and other TTS by Kenyon and Hartmann (1987, hereafter referred to as KH), Bertout *et al.* (1988, hereafter referred to as BBB), and Basri and Bertout (1989, hereafter referred to as BB). In such models there are four components to the predicted spectral energy distribution: (a) the photospheric radiation of the star itself, which dominates the spectrum—at least for BP Tau and other mild TTS—between 5000 and 9000 Å; (b) the accretion luminosity of the disk, which is important only at near infrared wavelengths; (c) the emission of the boundary layer of the disk, which accounts for half the total accretion luminosity and which dominates at UV wavelengths, where it hides the stellar spectrum; and (d) the “reprocessed” light from the star (or the inner portion of its disk), which is absorbed by dust grains in the outer regions of the disk before it finally emerges at thermal infrared wavelengths.

The accretion disk model posits that the UV excess and bright permitted emission lines of TTS form in the boundary

^{a)} Guest Observer with the *International Ultraviolet Explorer (IUE)* Satellite.

layer of the disk, just above the stellar surface. The physical structure of the boundary layer is essentially unknown. It is expected to be a narrow region, with a radial extent of no more than a few percent of the stellar radius (making it similar in size to a high pressure stellar chromosphere), and to be warm, but not hot. In the optically thick model computed by BBB for BP Tau, the temperature of the boundary layer is 8170 K; in the optically thin model of BB, the temperature is 8800 K. In either case, the boundary layer and disk temperatures in the models are far too low to produce the x-ray emission observed for BP Tau by Walter and Kuhi (1981) or the high-temperature UV lines discussed in this paper.

In the chromospheric model, the regular variability of a TTS can be explained by inhomogeneities on the surface of a star that undergoes rotation. Accretion models have thus far ignored this aspect of TTS behavior. It may be possible to accommodate stellar variability within accretion models by invoking nonsteady infall through the disk and its boundary layer. However, since the accretion models assume Keplerian motion, one would expect the characteristic timescale for variability in the disk to be comparable to the dynamical timescale and hence to be extremely short. In the case of BP Tau (for which we adopt $M \approx 0.8 M_{\odot}$ and $R \approx 2.5 R_{\odot}$), for example, the orbital period of the boundary layer is ~ 12 h, which is obviously much shorter than the 7.6 day photometric cycle observed by Vrba *et al.* (1986). On the other hand, orbital periods as long as 7.6 days are reached in the models only at very large radial distances within the disk where the temperature is < 1100 K and is therefore too low to contribute to the observed variability. Consequently, it may prove difficult to reconcile accretion disk models with the timescale of the variability actually observed for BP Tau and other periodic TTS.

The intent of this paper is to present new optical and UV observations of BP Tau that bear directly on this issue. Included here are UV spectra from the *International Ultraviolet Explorer (IUE)* satellite, which we obtained in October 1986 in order to study the possible time variability of high-temperature emission lines in the UV as well as the short-wavelength portion of the Balmer continuum that is inaccessible from the ground. In conjunction with the *IUE* observations, we also obtained supporting ground-based photometry. Most of these data were acquired in the weeks just following the *IUE* observing. Unfortunately, this lack of coincidence introduces major uncertainties in the analysis, as the subsequent discussion will show. In addition, since a limited amount of satellite time was available for this program, the UV observations sample only a few phases in the complete light cycle of BP Tau. However, since we have been unable to gain further observing time on *IUE* to follow up on these initial results, we have elected to present our findings here.

II. OBSERVATIONS

a) Ground-Based Photometry

$UBVR_c I_c$ photometry of BP Tau was obtained with the 1.0 m telescope of the Flagstaff Station of the U.S. Naval Observatory (USNO) on 10 nights between 25 October and 25 November 1986. The observations overlap the *IUE* observations by a single day, but the majority were acquired after the latter had ended. Observations in $VR_c I_c$ were made with the 0.6 m telescope of the Van Vleck Observatory (VVO) on 15 nights between 7 October and 23 November. These measurements overlap all but the first five days of the UV moni-

toring program. Our UBV results are on the standard Johnson (1966) system, while our R_c and I_c measurements are on the Cousins (1980) system. Previous experience (e.g. Herbst *et al.* 1986) shows that the USNO and VVO natural systems are closely matched, and since we used the same comparison star for BP Tau at both sites, we have combined the separate photometry of the BP Tau without further transformation.

Both sets of data are listed in Table I. The observational errors are typically 0.01 mag in all filters. A comparison of these measurements with our earlier photometry of BP Tau from October 1983 (Vrba *et al.* 1986) reveals only minor changes in the amplitude of the variability at each wavelength and in the slopes of the color vs V -magnitude relations (Vrba *et al.* 1985) over the intervening three years.

As we did in our earlier study, we have used the periodogram technique of Scargle (1982) to search for periodicity in each of the individual light curves. This time, however, unlike 1983, we do not find one dominant peak in the power spectra computed from the photometry. Rather, there are several peaks at different frequencies corresponding to periods ranging from 5.95 to 7.65 days, except that none of these periods yields a tight sinusoidal fit to the phased observations.

The reason for this difficulty can be understood from an inspection of Fig. 1, which shows a plot of the V magnitude against time. Shown here are the USNO and VVO measurements, along with the color-corrected V magnitude from the Fine Error Sensor (FES) of *IUE*, to which we have added a zero-point correction of 0.25 mag in order to adjust the spacecraft data to the VVO scale. Prior to JD 2446728 the data are compatible with a sine curve having a period of 7.6 ± 0.2 days. This is the same period established by Vrba *et al.* (1986) in a much larger dataset taken in October 1983. Thereafter, during a 12-day hiatus starting on JD 2446728, the star maintained constant brightness. The variability then resumed at JD 2446740, but with a new period of 6.1 ± 0.2 days. The same pattern is present in the R_c and I_c light curves, while the B and U data exhibit only the 6.1 day variation, since the latter measurements were all made after JD 2446728 (see Fig. 2). It appears, then, that the light curve of BP Tau evolved quite rapidly during our campaign, and that this instability accounts for the multiple peaks in the power spectra at V , R_c , and I_c .

If this photometric behavior is due to the decay and reformation of starspots at different latitudes on the surface, then the difference between the 7.6 and 6.1 day periods implies that BP Tau must have a surface differential rotation rate of at least 20%. This result invites comparison with other stars of similar mass. The position of BP Tau in the H-R diagram, when compared with theoretical evolutionary tracks (cf. Vrba *et al.* 1986), indicates that it is a star of $M \approx 0.7-1.0 M_{\odot}$. Published photometric rotation periods, at different epochs, of several stars in the same mass range show rotation periods differing by at least 10%. Examples include the TTS DN Tau (Vrba *et al.* 1986; Bouvier, Bertout, and Bouchet 1986b) and the "naked" T Tauri star V826 Tau (Rydgren *et al.* 1984; Bouvier and Bertout 1989). Among fully evolved stars of comparable mass, we note that the Sun has a surface differential rotation rate of approximately 20% between the equator and latitude 60° , which becomes even greater at higher latitudes (Snodgrass 1983). Thus, the differential rotation we infer for BP Tau is not inconsistent with results for other low-mass stars.

TABLE I. Summary of ground-based photometry.

JD- 2440000	Magnitudes				
	U	B	V	R _c	I _c
a) U.S. Naval Observatory					
6728.776	13.636	13.486	12.194	11.294	10.440
6728.937	13.752	13.462	12.164	11.268	10.403
6729.793	13.876	13.526	12.187	11.288	10.427
6729.974	...	13.506	12.177
6739.758	13.087	13.207	12.127	11.279	10.429
6739.956	13.048	13.198	12.151	11.311	10.465
6740.789	13.151	13.311	12.189	11.336	10.483
6741.006	12.918	13.148	12.095	11.274	10.462
6743.815	13.380	13.480	12.246	11.365	10.475
6743.982	13.608	13.488	12.253	11.351	10.488
6744.741	13.659	13.509	12.241	11.379	10.497
6744.920	13.683	13.523	12.277	11.396	10.529
6745.736	13.525	13.425	12.212	11.346	10.477
6745.992	13.621	13.491	12.254	11.362	10.501
6746.773	13.084	13.164	12.074	11.230	10.417
6746.990	13.048	13.168	12.060	11.216	10.380
6747.722	13.097	13.167	12.047	11.210	10.388
6747.978	12.903	13.033	11.995	11.198	10.337
6759.693	12.920	13.070	12.058	11.259	10.465
6759.931	12.901	13.061	12.029	11.228	10.421
b) Van Vleck Observatory					
6710.800	11.98	11.20	10.38
6711.800	11.94	11.14	10.27
6713.800	12.17	11.27	10.42
6715.700	12.18	11.28	10.43
6723.800	11.85	11.09	10.30
6728.800	12.20	11.29	10.41
6732.800	12.22	11.32	10.44
6734.800	12.16	11.31	10.44
6735.700	12.18	11.29	10.42
6737.800	12.18	11.28	10.44
6744.700	12.21	11.33	10.44
6748.700	12.13	11.30	10.44
6749.700	12.12	11.32	10.48
6756.800	12.23	11.38	10.50
6757.800	12.28	11.39	10.50

b) Ultraviolet Spectroscopy

We obtained UV spectra of BP Tau with the *IUE* satellite on six dates between 2 October and 27 October 1986. Table II is a list of all the images we acquired. Included here are three spectra of the sky background near BP Tau, which we took for a study of the 1215 Å Lyman α emission line and which we omit from further discussion. On four occasions we obtained low-dispersion spectra with both the short wavelength (SWP: 1200–2000 Å) and long-wavelength (LWP: 2000–3200 Å) cameras. On two other dates, the observations were confined to the LWP camera, but were made at both high and low dispersion. The exposure times were chosen to provide well-exposed spectra of various high-temperature lines in the SWP range (e.g., C IV 1550 Å), of the Mg II h and k lines near 2800 Å in the LWP range, and of the short- and long-wavelength ends of the LWP camera, where the sensitivity of *IUE* is relatively poor. All our observations were made through the Large Science Aperture.

To illustrate the significant changes that occurred in the UV spectrum of BP Tau, we present four spectra of this star in Fig. 3. The top panels correspond to the first two dates in Table II and show the spectrum only four days apart. Since this time interval is equal to half the 7.6 day photometric period, we will henceforth refer to these spectra as observations from cycle 1. After a lapse of 11 days, we repeated the observations in the next following cycle, at times which correspond to the beginning and the middle of the third photometric cycle in sequence. These spectra from cycle 3 are shown in the bottom panels of the figure. There can be no doubt that the UV spectrum of BP Tau is much brighter at the middle than at the start of each cycle. The $V(FES)$ magnitudes listed in Table II indicate that the visible luminosity of BP Tau followed the same pattern, becoming brighter at midcycle.

The UV spectra of BP Tau were calibrated, corrected for camera blemishes and cosmic-ray hits, and measured at the

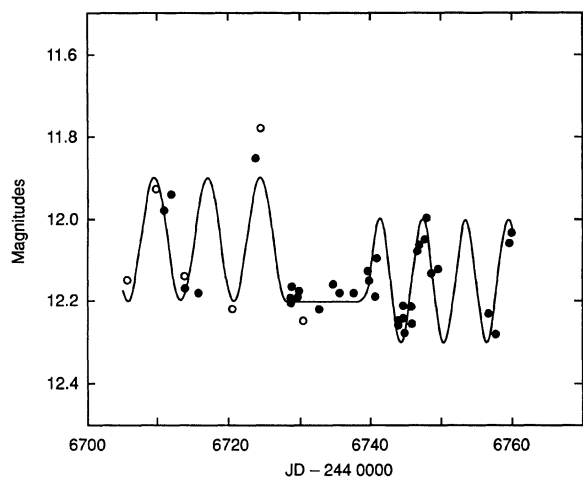


FIG. 1. V magnitude vs time for BP Tau. The open circles are the FES measurements from *IUE*, increased by a zero-point correction of 0.25 mag. Random errors in these measurements are estimated to be 0.05 mag. The solid dots are ground-based observations from the USNO and VVO. The sinusoid plotted here has a 7.6 day period prior to JD 2446728 and 6.1 day period after JD 2446740.

Regional Data Analysis Facility (RDAF) of the Goddard Space Flight Center with standard RDAF software. For the SWP spectra, we used the FEATURE program to measure the integrated flux of each prominent emission line above a local continuum level, which we set by eye with a graphics terminal. These results are given in Table III. The principal measurements made of the LWP spectra include the integrated flux of the Mg II emission lines and the average flux levels of the continuum. For the two high-dispersion LWP spectra acquired at the end of cycle 1 and cycle 3, we used the standard echelle grating constants to splice together overlapping orders of the spectrum near the Mg II h and k lines. We then

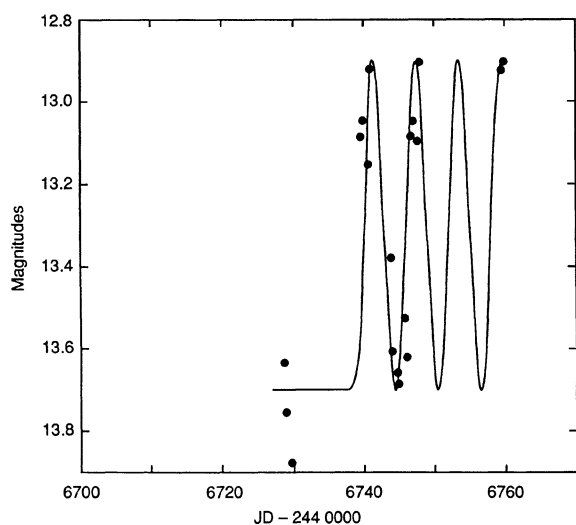


FIG. 2. Ground-based U band photometry of BP Tau vs time. A sine curve with a period of 6.1 days is plotted for comparison.

measured the integrated fluxes of the h and k emission features above the zero flux level.

In the low-dispersion LWP spectra, the stellar continuum is comparatively bright at 2800 Å. We therefore adopted several different procedures to measure the strength of the Mg II doublet (at low resolution the h and k components are blended). First, we used the FEATURE program to measure both the total line emission above the zero flux level as well as the net line flux above the adjacent continuum. These results are listed in columns 3 and 4, respectively, of Table IV. The net line flux in column 4 is expected to give the better estimate of a chromospheric energy loss; the total flux serves as an upper limit on that emission. We next estimated the height of the continuum at the Mg II lines by interpolating between 50-Å-wide continuum “windows” on either side of the Mg II lines. According to Herbig and Goodrich (1986), the 50 Å regions centered on 2700 and 3050 Å are as free of spectral lines as any portion of a TTS LWP spectrum ever gets. Using the RDAF program BINS, we determined the average flux levels in these “windows” and we then interpolated the continuum level to 2800 Å. This procedure occasionally resulted in a slightly lower continuum and higher line flux than before. The difference is illustrated in Fig. 4, where the white area under the Mg II feature is the flux measured by FEATURE above the continuum set with a graphics terminal (column 4 of Table IV), and the stippled area is the line flux added with a lower continuum level from BINS (column 5).

If one takes the view that there are no truly line-free windows in the LWP spectra of TTS, then perhaps the least objectionable place to draw the continuum is through the lowest points in the spectrum. Following this precept, and taking the analysis of T Tauri’s spectrum by Brown *et al.* (1984) as a guide, we used the RDAF program GNORM to fit a low-order polynomial to the lowest points in our deep LWP exposures. We then transferred this continuum level to the short exposures (from the same date) and measured the Mg II emission above this continuum. An example of this procedure is given in Fig. 4, which shows the fitted continuum and the incremental flux produced. The resulting line fluxes for the entire set of LWP spectra are listed in column 6 of Table IV under the heading GNORM.

Additional measurements were made of the SWP and LWP spectra to determine the average “continuum” flux levels in 50 Å bins throughout the UV. Admittedly, even in regions of these low-resolution spectra where no obvious spectral features are present, there may be many unresolved lines that make it impossible to find the true continuum flux levels. However, our chief interest here is in the variable component of the veiling emission, which may have an energy distribution that is effectively continuous. Whether or not this is true depends on the nature of its source, which is currently a matter of dispute. (Various accretion disk models assume, for example, that the boundary layer region radiates in the UV as a warm blackbody, as a conventional stellar photosphere, or as an isothermal slab of negligible-to-small optical thickness.) In order to expose both ends of the LWP camera properly for these continuum measurements, we took deep exposures at the beginning and middle of cycles 1 and 3 (i.e., at minimum and maximum light), at the cost of saturating the Mg II lines in these images due to the small dynamic range of the *IUE* Vidicon (Boggess *et al.* 1978).

The continuum measurements for both cycles are listed in Table V, along with fluxes based on our $UBVR_c I_c$ photome-

TABLE II. Journal of *IUE* observations.

<i>IUE</i> Image	Elapsed UT Day 1986	JD- 2440000	Exp. (Min).	V (FES)	Notes
L9227	274.924	6705.424	20	11.92	
L9228	275.053	6705.553	20	11.93	
S29345	275.063	6705.563	330	11.92	
L9229	275.232	6705.732	105	11.95	
S29346	275.282	6705.782	20		
L9230	275.309	6705.809	20	11.88	1
L9230	275.329	6705.829	20		1
L9231	275.366	6705.866	18	11.82	
L9254	278.910	6709.410	20	11.67	
L9255	279.038	6709.538	18	11.69	
S29382	279.056	6709.556	330	11.63	
L9256	279.232	6709.732	105	11.64	
S29383	279.286	6709.786	170		2
L9257	279.317	6709.817	18	11.73	
L9258	279.357	6709.857	18	11.70	
S29412	283.125	6713.625	255		2
L9282	283.129	6713.629	270	11.92	3
L9283	283.254	6713.754	18	11.92	
L9284	283.310	6713.810	75	11.87	
L9285	283.365	6713.865	14	11.86	
L9336	289.924	6720.424	18	11.98	
S29457	290.062	6720.562	285	11.97	
L9337	290.181	6720.681	45	11.95	
L9375	293.932	6724.432	18	11.68	
S29493	294.051	6724.551	300	11.67	
L9376	294.184	6724.684	62	11.23	
L9416	299.940	6730.440	18	12.04	
S29538	300.064	6730.564	260		2
L9417	300.066	6730.566	270	12.01	3
L9418	300.190	6730.690	18	11.95	

Notes: (1) Two spectra obtained at different positions within large aperture on same image.
(2) Image of sky background near BP Tau.
(3) High dispersion.

try from JD 2446740 onward. To convert the visible magnitudes to absolute fluxes, we adopt the flux calibrations of Johnson (1966) and Bessell (1979). Also listed in Table V are the dereddened fluxes that follow from an extinction correction of $A_v = 0.6$ mag (Cohen and Kuhl 1979) and the Taurus reddening law of Herbig and Goodrich (1986). Because A_v is small, the standard interstellar extinction curve gives nearly the same corrected fluxes.

A graphical summary of these measurements is presented in Fig. 5. The top panel shows the fluxes measured for the strongest lines in the SWP and LWP spectra as a function of time, while the bottom panel shows the time dependence of the visible and UV continuum. The curve labeled TR represents the sum of the transition region lines of N V, Si IV, and C IV. The V-band continuum flux is based on the FES magnitudes given in column 5 of Table II, without any zero-point adjustment. The UV continuum flux is taken from the measurements with FEATURE, since a comparison of the total

UV brightness, with any possible emission lines included, may be the most relevant comparison here. The optical and UV continua varied in phase with the same pattern in both cycles, increasing in brightness from minimum brightness at the start of each cycle to maximum brightness at midcycle. All of the emission line strengths also increased from the start to the midpoint of both cycles. However, the measurements taken of Mg II at the end of cycle 1 and at the end of cycle 3, on dates when no SWP spectra are available, appear to illustrate a significantly different behavior, which we will discuss in the following section.

III. DISCUSSION

a) Variable Circumstellar Extinction

Of the many proposals that have been made to explain the photometric variability of TTS, we consider first whether variable circumstellar extinction (cf. Gahm *et al.* 1974) can

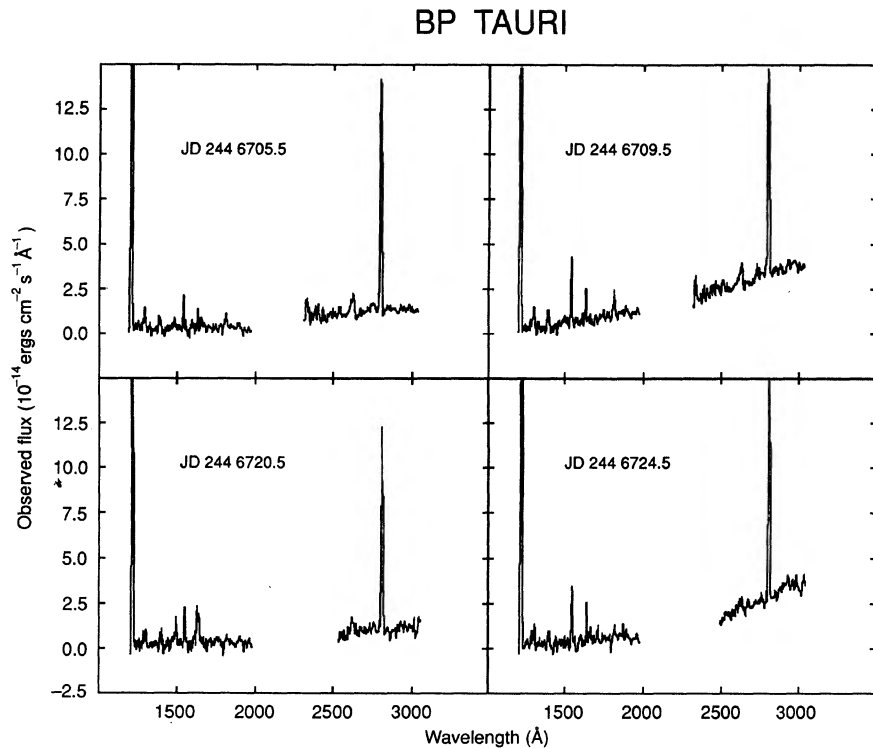


FIG. 3. *IUE* spectra taken a half-period apart during two rotation cycles of BP Tau. The top panels refer to cycle 1, the bottom pair to cycle 3. The bright Ly α emission feature on the left-hand side of each spectrum is contaminated by geocoronal emission. The strong emission line at 2800 \AA is the blended doublet of Mg II. The other prominent emission features are spectral lines of O I, C II, C IV, C II], and Fe II.

account for the observed amplitude of the optical and UV variations of BP Tau. From the information provided in Tables I and V we compute the ratio of the fluxes observed at maximum and minimum light within each light cycle. We express the amplitude in magnitudes by computing $2.5 \log (f_{\max}/f_{\min})$, and we then plot the average value of this quantity for cycles 1 and 3 as a function of wavelength in Fig. 6. Starting at visible wavelengths, the amplitudes increase steeply into the UV range observed by *IUE*, whereupon the trend becomes more uncertain. A weighted least-squares fit to the UV amplitudes suggests that the variability may diminish at the shortest wavelengths, but the error bars below 2000 \AA (indicating the differences recorded between the two cycles) are quite large. To within the errors, a constant amplitude of 0.96 mag provides nearly equally good fit to the *IUE* measurements.

If the presumed variable component of the circumstellar extinction of BP Tau follows the Taurus extinction law given by Herbig and Goodrich (1986), it is a simple matter to

calculate the amplitude expected at each wavelength, given the observed amplitude of 0.3 mag at 5500 \AA . The resulting values, normalized at V, are drawn as open boxes in Fig. 6. The predicted rise toward UV wavelengths is clearly much weaker than the observed trend. The discrepancy is especially large at 3000 \AA , where the observational errors are small. We therefore conclude that the variability of BP Tau is unlikely to be caused by variable dust extinction unless the circumstellar grains obscuring this star are $\sim 60\%$ more opaque at short wavelengths than are normal interstellar grains. Although there can be significant differences in the properties of cosmic dust grains, depending on their chemical composition and size, we have no other evidence to indicate that the grains around BP Tau are anomalous.

b) Boundary Layer Radiation Due to Accretion

An accretion disk model was computed specifically for BP Tau by BBB, who derived a boundary layer temperature of

TABLE III. Measurements of UV line fluxes (10^{-14} ergs cm^{-2} s^{-1}).

SWP	JD - 2440000	N v λ 1240	O I λ 1304	C II λ 1335	Si IV λ 1400	C IV λ 1550	He II λ 1640	C I λ 1657	Si II λ 1810	Si III λ 1892
29345	6705.563	1.32 ^a	10.0	3.75	13.1	13.5	8.22	—	9.14	2.71
29382	6709.556	1.53 ^a	15.8	5.79	17.6	26.7	13.7	—	18.2	3.35
29457	6720.562	1.50 ^a	8.88	1.03	12.1	18.6	11.9	—	5.20	3.66
29493	6724.551	1.02 ^a	9.11	2.45	13.0	24.7	13.7	3.77 ^a	4.90	3.11

^a Uncertainty in measured flux estimated to be $\sim 30\%$. Errors in the remaining measurements are on the order of 15% or less.

TABLE IV. Measurements of Mg II line flux (10^{-14} ergs cm^{-2} s^{-1})^a.

LWP	JD- 2440000	Line Flux Above Zero	Line Flux Above Continuum From:		
			FEATURE	BINS	GNORM
9227	6705.424	219	183	181	187
9228	6705.553	218	176	170	184
9229	6705.732	>131	>86	>91	>99
9230 ^b	6705.819	191	157	156	165
9231	6705.866	216	171	169	188
9254	6709.410	324	209	200	215
9255	6709.538	317	191	179	197
9256	6709.732	>175	>63	>65	>72
9257	6709.817	259	168	162	182
9258	6709.857	296	187	192	192
9282 ^c	6713.629	273
9283	6713.754	335	274	265	282
9284	6713.810	>196	>129	>130	>145
9285	6713.865	322	268	259	279
9336	6720.424	156	127	123	142
9337	6720.681	>163	>131	>123	>143
9375	6724.432	226	165	165	165
9376	6724.684	>218	>119	>114	>128
9416	6730.440	208	186	184	193
9417 ^c	6730.566	178
9418	6730.690	217	188	185	201

^a Uncertainties in the measurements are in all cases <5%.

^b Total exposure time is 40 minutes.

^c High dispersion.

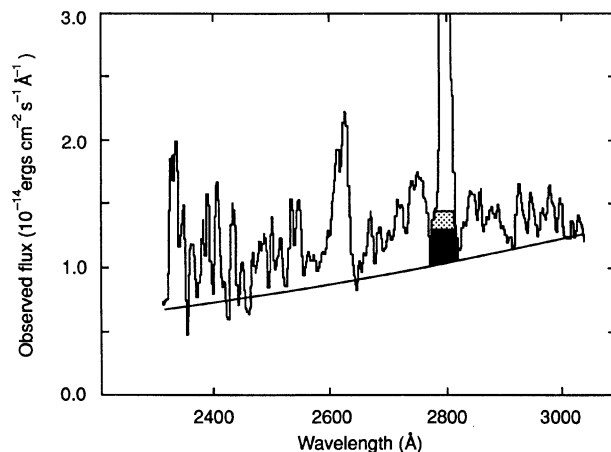


FIG. 4. Measurements of the Mg II emission feature in a low-dispersion *IUE* spectrum (LWP 9229) assuming three different continuum levels. The white area within the emission feature corresponds to the net flux measured above a continuum drawn through the middle of the peaks and valleys in the spectrum near 2800 Å. The stippled area is the additional line flux measured when the continuum level at 2800 Å is interpolated between two 50-Å-wide “windows” centered at 2700 and 3050 Å. The dark area is the line flux gained when the continuum is a polynomial curve placed through the lowest points in the spectrum, as shown by the heavy solid line.

8170 K by fitting a blackbody curve to contemporaneous UV and optical spectra taken in 1983. We present a similar fit to our observations in Fig. 7. To within the observational uncertainties, the blackbody curve matches the dereddened 1700–3100 Å flux distribution of BP Tau reasonably well at both maximum and minimum light in the two cycles we have observed. However, an extrapolation of the curve to longer wavelengths predicts an enormous excess in the *U* and *B* filters as well as strong veiling that, at maximum light, extends as far longward as 5500 Å. By comparison, the observations of BBB exhibit at most a small Balmer jump [see their Fig. 6(a)] and the boundary layer in their accretion disk model contributes no more than a third of the total flux at 5500 Å. Hartigan *et al.* (1989) have estimated from independent observations of BP Tau that the veiling continuum represents less than one-half the total light in the 5100–6600 Å region.

Our results therefore imply a much higher degree of veiling at visible wavelengths than other studies have found in the past. Since our optical and UV observations were not strictly simultaneous, it may be possible to account for this discrepancy if BP Tau was substantially brighter at visible wavelengths at the time of our *IUE* observations than during the interval following JD 2446740, when the optical energy distribution shown in Fig. 7 was measured. To reduce the amount of veiling near 5500 Å to < 50% at maximum light,

TABLE V. Continuum flux measurements (10^{-14} ergs cm^{-2} s^{-1} \AA^{-1})^a.

λ (\AA)	C_{λ} ^b	Cycle 1				Cycle 3			
		Observed Flux		Dereddened Flux		Observed Flux		Dereddened Flux	
		Min.	Max.	Min.	Max.	Min.	Max.	Min.	Max.
1750	4.41	0.28	1.10	1.24	4.85	0.47	0.62	2.07	2.73
1925	4.23	0.22	1.23	0.93	5.20	0.30	0.61	1.27	2.58
2450	3.69	1.00	2.71	3.68	10.01	0.70	1.65	2.58	6.08
2500	3.65	1.19	2.85	4.33	10.41	...	1.77	...	6.45
2550	3.61	1.10	2.64	3.97	9.54	0.76	2.06	2.73	7.44
2600	3.57	1.39	3.14	4.98	11.20	1.16	2.44	4.13	8.73
2650	3.53	1.30	2.93	4.60	10.37	1.13	2.55	4.00	8.99
2700	3.49	1.24	3.09	4.31	10.79	1.08	2.58	3.76	9.01
2750	3.46	1.54	3.38	5.32	11.71	1.19	2.80	4.13	9.70
2800	3.42
2850	3.38	1.32	3.40	4.46	11.49	1.00	3.17	3.36	10.71
2900	3.35	1.39	3.59	4.64	12.04	1.15	3.67	3.86	12.30
2950	3.31	1.48	4.06	4.92	13.44	1.27	3.75	4.19	12.42
3000	3.27	1.47	3.85	4.81	12.60	1.23	3.61	4.02	11.80
3050	3.25	1.34	3.43	4.36	11.12	1.25	3.70	4.06	11.98
3600	2.51	1.50	3.00	3.80	7.55	1.50	3.00	3.80	7.55
4400	1.96	2.80	4.40	5.50	8.60	2.80	4.40	5.50	8.60
5500	1.75	4.80	6.20	8.40	10.85	4.80	6.20	8.40	10.85
6400	1.60	6.70	7.90	10.70	12.65	6.70	7.90	10.70	12.65
7900	1.40	7.60	9.10	10.70	12.75	7.60	9.10	10.70	12.75

^a The *IUE* fluxes are averaged over 50- \AA bins centered on the wavelengths indicated. The fluxes at visible wavelengths are based on the photometry acquired after JD 2446740. We estimate the uncertainties in the UV fluxes to be as follows: *LWP*, 5% in Cycle 1 and 10% in Cycle 3; *SWP*, 20% at light maximum and 35% at light minimum.

^b Correction for extinction following the Taurus reddening curve of Herbig and Goodrich (1986), $A_{\lambda} = 2.5 \log C_{\lambda}$.

however, requires an adjustment of almost 0.5 mag in *V*. This is far more than we consider reasonable, since it is unlikely according to Fig. 1 that BP Tau was as bright as $V = 11.5$ mag at any time during the course of our *IUE* observations. In fact, archival photometry shows that in recent times BP Tau has never been as bright as $V = 11.5$ (Rydgren *et al.* 1984).

An alternative explanation for this discrepancy is simply that the Balmer continuum is optically thin. More than a decade ago, Rydgren *et al.* (1976) showed that the veiling of many TTS energy distributions is consistent with a hydrogen recombination spectrum from a hot (20 000 K), optically thin envelope, which they suggested to be the principal source of the irregular light variations of these stars, and more recently, BB have presented an optically thin boundary layer model for BP Tau in place of the optically thick model of BBB.

Prompted by Walker's (1987) suggestion that the UV excess for some TTS might originate in an independent source of continuous emission, we focus attention here on the *vari-*

able component of BP Tau's spectral energy distribution. Based on the information provided in Table V, we have computed the difference in flux observed between the maximum and minimum brightness and have averaged the results for cycles 1 and 3. The mean differences are plotted as a function of wavelength in Fig. 8. The shaded circles refer to the observed fluxes, while the open circles are the values dereddened for $A_{\nu} = 0.6$ mag. For comparison with the UV and optical flux differences, Fig. 8 also shows an optically thin, hydrogen recombination spectrum (free-bound and free-free), which we have computed for a plasma temperature of 13 000 K. The computed spectrum is normalized to the observed and dereddened spectral energy distributions near 3100 \AA .

The shape of the Balmer continuum of the model and the UV flux difference curve measured by *IUE* are in excellent agreement. However, the predicted Balmer jump is clearly too large and the predicted emission in the Paschen continuum is much less than the flux we have observed. Although the discrepancies can be reduced if we raise the envelope

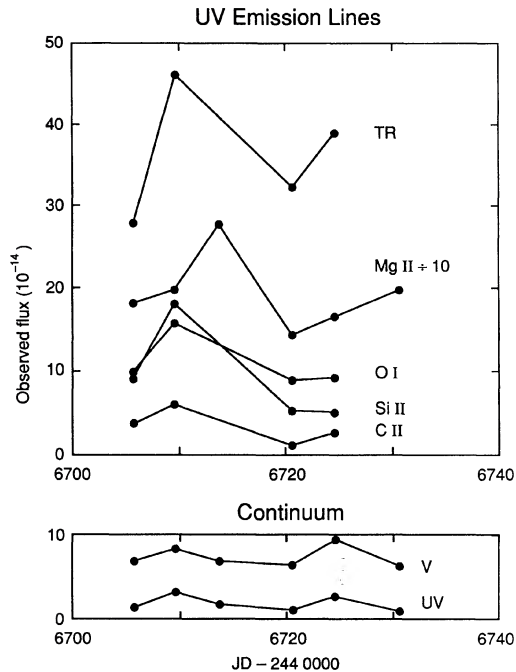


FIG. 5. The net flux for UV emission lines observed at the Earth is plotted as a function of time in the top panel. The bottom panel shows light curves for the 5500 Å continuum flux, derived from the FES magnitudes, and the 2800 Å UV continuum flux, based on measurements made with the computer program FEATURE. TR denotes the sum of the fluxes of N V (1240 Å), Si IV (1400 Å), and C IV (1550 Å). Mg II denotes the average flux computed for each date from the entries in the column headed GNORM in Table IV. The uncertainties in the line fluxes (other than Mg II) are typically 15%, corresponding to a 1σ error bar approximately the same height as the Roman numerals drawn in the figure, while the uncertainties in Mg II are 5% or less, giving error bars that are smaller than the dots shown. The uncertainties in the average V and UV continuum flux are typically 2% and 5%, respectively.

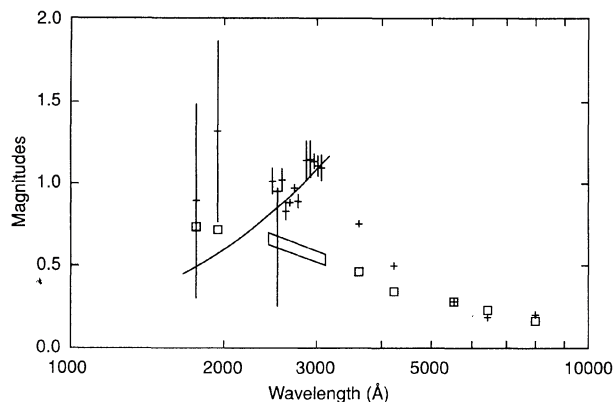


FIG. 6. Amplitude of the light variations of BP Tau as a function of wavelength. Plotted here is the average amplitude in magnitudes for cycles 1 and 3, $\langle 2.5 \log(f_{\max}/f_{\min}) \rangle$. The range in amplitude from one cycle to the next is indicated by the error bars. The solid curve is a weighted least-squares fit to the UV amplitudes below 3600 Å. The open boxes are the amplitudes predicted by the Taurus reddening law, assuming a variation of 0.3 mag in V .

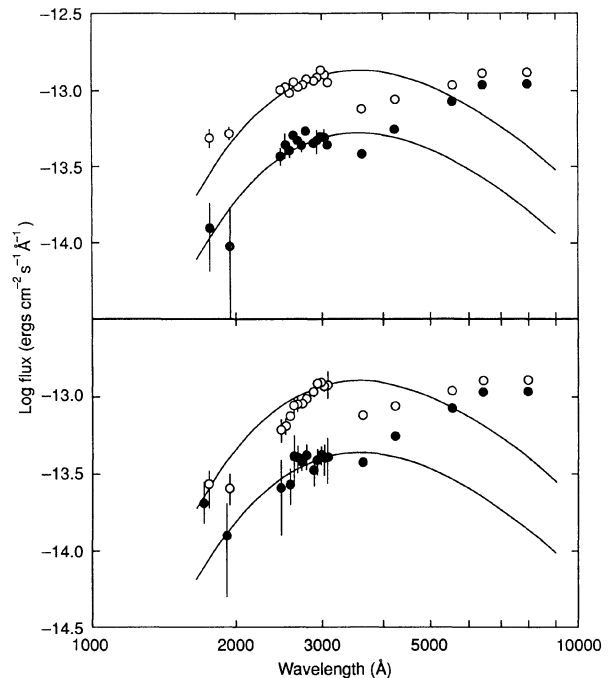


FIG. 7. Comparison of a blackbody spectrum for an optically thick boundary layer with the dereddened spectral energy distribution of BP Tau at light maximum (open circles) and light minimum (shaded circles) for cycle 1 (top panel) and cycle 3 (bottom panel). The blackbody curve corresponds to a temperature of 8170 K and is scaled to the *IUE* flux at 3000 Å, where the UV line emission is minimized. Error bars are shown only when they exceed the size of the symbol. The fluxes are from Table V.

temperature above 13 000 K, the temperature is tightly constrained by the short-wavelength UV fluxes below 2000 Å, even with their large errors. On the other hand, the discrepancy in the strength of the Balmer jump and the Paschen continuum is increased if we assume (as before) that BP Tau was brighter at visible wavelengths during the *IUE* observations than during the following period. A likely explanation for these difficulties is that the Balmer continuum has an

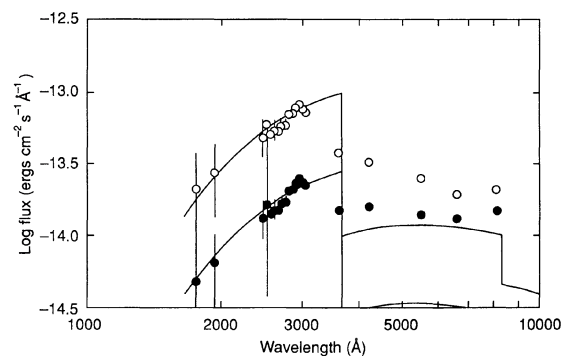


FIG. 8. Difference in flux between minimum and maximum light as a function of wavelength. The open circles represent the dereddened fluxes and the shaded circles denote the observed values. Shown here is the average of the flux differences for cycles 1 and 3, with error bars to indicate the change in amplitude between cycles. Also plotted is the flux distribution expected for an optically thin hydrogen recombination spectrum at a temperature of 13 000 K.

optical depth of order unity, as BB have suggested for their accretion disk model of BP Tau. Further calculations, taking such optical depth effects into account, are beyond the scope of this study until the ambiguities in the visible light curves cited earlier can be resolved.

c) *The Timescale for Variability*

Given the very limited phase coverage of our *IUE* observations, we are unable to demonstrate that any changes in the UV spectrum of BP Tau are truly periodic. Nevertheless, as is apparent from Fig. 5, the changes we have observed are clearly systematic and are at least not inconsistent with periodic behavior.

Within the framework of the deep chromosphere model, the photometric cycle of 7.6 days exhibited by BP Tau in 1983, and possibly during the course of our *IUE* observations, can be interpreted as the rotation period of this star. If this view is correct, then the $v \sin i < 10 \text{ km s}^{-1}$ measured by Hartmann *et al.* (1986) and the radius of $2R_{\odot} \leq R < 3R_{\odot}$ typically assumed for this star (cf. BBB and BB) together suggest that BP Tau is viewed at low inclination, $i < 48^{\circ}$ for $R = 2R_{\odot}$ or $i < 30^{\circ}$ for $R = 3R_{\odot}$. Presumably the onset of a nearly 6-day cycle after JD 2446740 is the result of the sudden decay of the initial bright starspot observed by *IUE* and the equally sudden emergence of a second spot at a different latitude having a faster rotation rate.

Such long timescales for the observed variability are difficult to reconcile with accretion disk models that produce UV emission in a boundary layer close to the very surface of a star. A boundary layer in Keplerian motion around a star of radius $2R_{\odot} \leq R < 3R_{\odot}$ is expected to have an orbital period of 9–16 h. If the variability we see arises from nonsteady accretion through the boundary layer (as the models of KH, BBB, and BB would seem to require), then the most likely characteristic timescale for such variability should be comparable to this dynamical timescale, which is of the same order as 1 or 2 *IUE* observing shifts. We find no evidence in our Mg II spectra for any significant (> 30%) variability in UV line or continuum emission on such short timescales (see Table IV). Moreover, a period of 7.6 days corresponds to a radial distance in the accretion disk models of $5R_{\odot}$, if $R = 3R_{\odot}$ and to $8R_{\odot}$, if $R = 2R_{\odot}$, at which distance the temperature of the disk is < 1100 K. Such temperatures are much too cold for the disk to radiate the high-temperature UV emission lines that we observe to vary on timescales as long as a week.

As for the Mg II lines, BBB have suggested that these lines may originate from a chromosphere associated with the boundary layer. The strength of Mg II possibly varies with a 15 day cycle, rather than the 7.6 day cycle of the continuum, but there is no strong evidence that Mg II varies on much shorter timescales ranging from a few hours up to half a day. Obviously it will be important to confirm this result by observing with better phase coverage and also to establish whether the other high-temperature lines in the SWP range vary with the same period as the continuum or with the even longer period of Mg II.

It is conceivable that the UV-emitting region rotates at a rate that is sub-Keplerian. One way to accomplish this has been suggested by Uchida and Shibata (1984, 1985), who

propose a “magnetically buffered” accretion model, in which material is suspended within the disk by magnetic tension until the magnetic field lines of the star and the disk reconnect. This allows material from the disk to flow down onto the magnetic polar regions of the star, where it crashes onto the surface to produce a strong shock having a temperature $\sim 10^6$ K. This temperature is high enough to generate x-ray emission as well as all of the high-temperature UV lines that cannot be produced in a 10^4 K boundary layer. In this magnetic accretion model, the UV emission produced at the hot polar crown of the star should be modulated by the rotation of the star and accordingly, for BP Tau, should vary on a ~ 7.6 day timescale if this star is not seen exactly pole-on. Superficially, such an accretion hot spot might closely resemble what we would otherwise label a “bright starspot.” A similar idea was suggested for the star DF Tau by BBB.

IV. CONCLUSIONS

In this paper we have presented ground-based optical photometry for BP Tau measured during 24 days of an approximately 50 day window during 1986, along with UV spectra measured with *IUE* during six days only partially in common with the optical data. We have been able to demonstrate from these data that BP Tau exhibited a periodic variation in optical brightness during a significant portion of the monitoring period, and that the UV continuum fluxes and most of the UV emission lines most likely varied in phase with the optical light.

Our results seem to preclude the variable circumstellar extinction hypothesis as the fundamental cause for the light variability of BP Tau during the observing period. Theoretical models of accretion disks or chromospheres can explain some features of the observed spectral energy distribution, while failing badly to explain others. [We have chosen not to present a detailed discussion of the chromospheric models as these results are specifically discussed for BP Tau by Calvet, Basri, and Kuhl (1984) and Calvet and Marin (1987).] Clearly, more realistic modeling is needed from both camps in order to explain well-known TTS spectral features. However, it may be that the biggest impediment to improving such models is still the lack of a suitable database upon which to build the models. Despite our best efforts, the limited phase coverage, particularly in the UV data obtained with *IUE*, remains a serious handicap to such studies. Future TTS optical and UV monitoring campaigns should therefore be directed toward intensive observations aimed at *full phase coverage* and with sufficient sampling to resolve the several-day timescale now known to be characteristic of TTS variability.

We thank the staff of the *IUE* Observatory for their assistance in the acquisition and reduction of the UV data presented. We also thank Chris Anderson and Wendy Nakano for their help in preparing the manuscript. The *IUE* research reported was supported by NASA Grant No. NAG 5-146 to the University of Hawaii.

REFERENCES

- Basri, G., and Bertout, C. (1989). *Astrophys. J.* **341**, 340 (BB).
- Bertout, C., Basri, G., and Bouvier, J. (1988). *Astrophys. J.* **330**, 350 (BBB).
- Bessell, M. S. (1979). *Publ. Astron. Soc. Pac.* **91**, 589.
- Boggess, A., *et al.* (1978). *Nature* **275**, 372.
- Bouvier, J., and Bertout, C. (1989). *Astron. Astrophys.* **211**, 99.
- Bouvier, J., Bertout, C., Benz, W., and Mayor, M. (1986a). *Astron. Astrophys.* **165**, 110.
- Bouvier, J., Bertout, C., and Bouchet, P. (1986b). *Astron. Astrophys.* **158**, 149.
- Brown, A., Ferraz, M. C. de M., and Jordan, C. (1984). *Mon. Not. R. Astron. Soc.* **207**, 821.
- Calvet, N., Basri, G., and Kuhl, L. V. (1984). *Astrophys. J.* **277**, 725.
- Calvet, N., and Marin, Z. (1987). *Rev. Mex. Astron. Astrof.* **14**, 353.
- Cohen, M., and Kuhl, L. V. (1979). *Astrophys. J. Suppl.* **41**, 743.
- Cousins, A. W. J. (1980). *S. Afr. Astron. Circ.* **1**, 234.
- Gahm, G. F., Nordh, H. L., Olofsson, S. G., and Carlborg, N. C. J. (1974). *Astron. Astrophys.* **33**, 399.
- Hartigan, P., Hartmann, L., Kenyon, S., Hewett, R., and Stauffer, J. (1989). *Astrophys. J. Suppl.* **70**, 899.
- Hartmann, L., Hewett, R., Stahler, S., and Mathieu, R. (1986). *Astrophys. J.* **309**, 275.
- Herbig, G. H. (1970). *Mem. R. Soc. Liege Ser. (5)* **9**, 13.
- Herbig, G. H., and Goodrich, R. W. (1986). *Astrophys. J.* **309**, 294.
- Herbst, W. (1989). *Astron. J.* **98**, 2268.
- Herbst, W., Booth, J. F., Chugainov, P. F., Zajtseva, G. V., Barksdale, W., Covino, E., Terranegra, L., Vittone, A., and Vrba, F. J. (1986). *Astrophys. J. Lett.* **310**, L71.
- Holtzman, J. A., and Herbst, W. (1986). In *Cool Stars, Stellar Systems, and the Sun*, edited by M. Zeilik and D. M. Gibson (Springer, New York), *Lect. Notes Phys.* **254**, 265.
- Johnson, H. L. (1966). *Annu. Rev. Astron. Astrophys.* **4**, 193.
- Kenyon, S. J., and Hartmann, L. (1987). *Astrophys. J.* **323**, 714 (KH).
- Kuhl, L. V. (1964). *Astrophys. J.* **140**, 1409.
- Rydgren, A. E., Schmelz, J. T., Zak, D. S., and Vrba, F. J. (1984). *Pub. U.S. Nav. Obs. Sec. Ser.* **XXV**, Part I.
- Rydgren, A. E., Strom, S. E., and Strom, K. M. (1976). *Astrophys. J. Suppl.* **30**, 307.
- Rydgren, A. E., Zak, D. S., Vrba, F. J., Chugainov, P. F., and Zajtseva, G. V. (1984). *Astron. J.* **89**, 1015.
- Scargle, J. D. (1982). *Astrophys. J.* **263**, 835.
- Snodgrass, H. B. (1983). *Astrophys. J.* **270**, 288.
- Uchida, Y., and Shibata, K. (1984). *Publ. Astron. Soc. Jpn.* **36**, 105.
- Uchida, Y., and Shibata, K. (1985). *Publ. Astron. Soc. Jpn.* **37**, 515.
- Vrba, F. J., Rydgren, A. E., Zak, D. S., and Schmelz, J. T. (1985). *Astron. J.* **90**, 326.
- Vrba, F. J., Rydgren, A. E., Chugainov, P. F., Shakovskaya, N. I., and Zak, D. S. (1986). *Astrophys. J.* **306**, 199.
- Vrba, F. J., Rydgren, A. E., Chugainov, P. F., Shakovskaya, N. I., and Weaver, W. B. (1989). *Astron. J.* **97**, 483.
- Walker, M. F. (1987). *Publ. Astron. Soc. Pac.* **99**, 392.
- Walter, F. M., and Kuhl, L. V. (1981). *Astrophys. J.* **250**, 254.